ELSEVIER

Energetics of intermolecular HONO formation in condensed-phase octahydro-1,3,5,7-tetranitro-1,3,5,7-tetrazocine (HMX)

James P. Lewis [*]

Department of Physics and Astronomy, Brigham Young University, N233 ESC P.O. Box 24658, Provo, Utah 84602-4658, USA

Received 24 January 2003; in final form 20 February 2003

Abstract

We present preliminary work on the formation of HONO in condensed-phase HMX for the three pure polymorphic phases. Our results show that the energetics of the intermolecular hydrogen transfer (to form HONO on an adjacent molecule) is more favorable in δ-HMX than in α-HMX and β-HMX. The energetics of this intermolecular hydrogen transfer process follow the same trends of HMX sensitivity, where δ-HMX is found to be more sensitive to explosion compared to β-HMX.
© 2003 Elsevier Science B.V. All rights reserved.

1. Introduction

While the history of highly energetic (HE) materials is long in both commercial and military aspects, the reaction mechanisms of decomposition pathways in these materials are not completely understood. A more detailed investigation of the kinetics and decomposition mechanisms is desired, but the instability of HE materials under high temperature and pressure regimes makes doing experimental work a difficult task. Information regarding HE decomposition is quite necessary in efficiently building the next generation of explosives as the quest for cheaper and yet more energetic materials (in terms of energy per density) moves forward. In addition, understanding the reaction mechanisms has important ramifications in decomposing such materials safely and cheaply, as there exist vast stockpiles of HE materials with corresponding contamination of earth and groundwater at these sites, as well as at military testing sites (for example, see [1,2]).

Numerous experimental studies investigate RDX/HMX decomposition and there exists a solid understanding of the putative rate limiting reaction (NO_2 dissociation) and the final products of the decomposition process (for example, see [3] and references therein). In addition, several theoretical studies investigating the energetics of gas-phase RDX/HMX decomposition pathways have been reported using a variety of methods both with quantum chemistry [4–8] and classical simulations

[*] Fax: 1-8014220553.
E-mail address: james_lewis@byu.edu.

of unimolecular dissociation [9–11]. More recently, condensed-phase simulations have been reported [12–14]; however, investigation of the energetics for a full reaction pathway in condensed-phase RDX/HMX near 'cook-off' conditions is still lacking.

An important consideration in understanding HMX decomposition is to evaluate the sensitivity-decomposition relationships that exist [15]. Post-mortem analysis [16] of samples recovered from safety experiments involving low-velocity projectile impacts on the HMX-based PBX-9501 [17] has revealed formation of δ-HMX in the vicinity of damaged regions within the material. It is also known that a layer of δ-HMX is formed at the solid-melt interphase in deflagrating HMX. These observations present a safety concern since δ-HMX is considerably more sensitive than β-HMX (i.e., δ-HMX is more likely to explode).

One of the more prevalent products of HMX decomposition is HONO. Formation of HONO can likely occur from unimolecular dissociation where the process of this reaction is an hydrogen transfer from the CH_2 group to the NO_2 group (see Scheme 1) [18]. However, the molecular packing in HMX would seem to suggest that hydrogen transfer can occur intermolecularly between adjacent molecules; there is a very weak hydrogen-bonding-like interaction from the C–H of the CH_2 group of one molecule to the O of the NO_2 group of its adjacent molecule.

In this work, we investigate the energetics of HONO formation in condensed-phase HMX, where intermolecular hydrogen transfer occurs. Results on the energetics of HONO formation in the three pure polymorphic phases (α, β, and δ) are presented here using our ab initio tight-binding method (called FIREBALL). We have previously

used the FIREBALL method to examine the energetics of the three pure polymorphic HMX phases [19]. In addition, the method has demonstrated good results for the dissociation of NO_2 in HMX (~34 kcal/mol [20] compared to ~37 kcal/mol experimentally [21], and between 33.0 and 39.8 kcal/mol found theoretically [5]).

2. Computational method

The theoretical basis of the FIREBALL method is the use of DFT with a nonlocal pseudopotential scheme. A summary of the method will be given here and we refer the reader to [22] and references therein for a more detailed description.

At the core of the method is a self-consistent density functional, where the input density is a sum of confined spherical atomic-like densities, $\rho_{in}(\mathbf{r}) = \sum_i n_i |\phi_i(\mathbf{r} - \mathbf{R}_i)|^2$. The orbitals $\phi_i(\mathbf{r} - \mathbf{R}_i)$ are the basis functions used in solving the one-electron Schrödinger equation. The occupation numbers n_i determine the number of electrons occupying each spherically confined atomic-like densities. The total energy is therefore a *function* of the occupation numbers, $E_{tot}[\rho_{in}(\mathbf{r})] \equiv E_{tot}[n_i]$ ($n_i \neq n_i^0$), and a self-consistent procedure on the occupation numbers, n_i, is introduced ($n_i = n_i^0 + \delta n_i$) [23]. For the exchange–correlation interactions [24] various parameterizations of the local-density approximation (LDA) and of the generalized gradient approximation (GGA) are available. For this work, we use the GGA form containing Becke exchange (B88) [25] with Lee–Yang–Parr (LYP) correlation [26].

In solving the one-electron Schrödinger equation a set of slightly excited pseudoatomic *fireball*
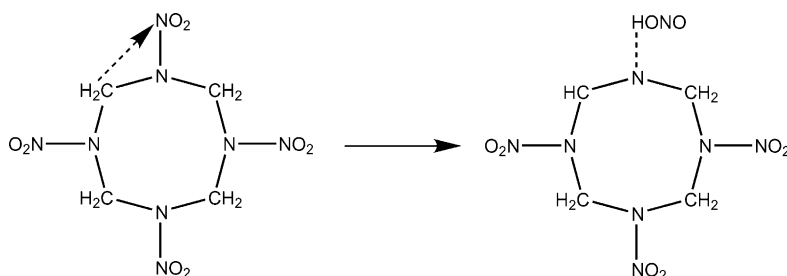
Scheme 1.

wavefunctions are used. These orbitals are computed within DFT and the generalized norm-conserving separable pseudopotentials of the Hamann form [27] are used, employing for their construction the scheme of Fuchs and Scheffler [28]. The pseudopotentials are transformed into the fully separable form suggested by Kleinman and Bylander [29]. The *fireball* wavefunctions are chosen such that they vanish at some radius r_c ($\psi_{\text{fireball}}^{\text{atomic}}|_{r \geqslant r_c} = 0$). This boundary condition is equivalent to an *atom in the box* and has the effect of raising the electronic energy levels ($\epsilon_s, \epsilon_p, \epsilon_d, \ldots$ atomic eigenvalues) due to confinement. The *fireball* boundary condition yields promising features. First, the slight excitation of the atoms somewhat accounts for Fermi compression in solids which apparently gives a better representation of solid-state charge densities [30]. Second, the range of hopping matrix elements between orbitals on different atoms is limited; therefore, very sparse matrices are created for large systems.

The radial cutoffs (r_c) are chosen such that these electronic eigenvalues remain negative and are mildly perturbed from the free atom – H ($r_c = 3.8$), C ($r_c = 4.1, 4.4$), N ($r_c = 3.7, 4.1$), and O ($r_c = 3.5, 3.8$) (for s and p shells, respectively). Double numerical (DN) basis sets for C, N, O are also included, as prescribed by Delley [31] where the wavefunctions of the 2^+ ions determine the excited state orbitals.

A simple barrier algorithm is used to estimate the energetic pathway by *pushing* the system of interest between an initial configuration and a final configuration through a path of least resistance. At each time step we take the vector difference, for each atom, between the current position (the first time step of the simulation is the initial configuration) and the final, or desired, configuration. These difference vectors are then transformed into unit vectors, which describe the direction that each atom must move in order to reach the final configuration. Next, we examine the calculated forces for each atom. The atoms are then moved in the direction of the force yielding a nonnegative component in the desired direction. This procedure insures that each atom always has some component of acceleration towards the desired final position of each atom.

3. Results and discussion

We use the barrier approximation as outlined in Section 2 for a first-order investigation of the intermolecular hydrogen transfer in condensed-phase HMX. The results presented here will be taken as a point of reference for future investigations where we perform simulations using umbrella sampling to refine the energetics of the intermolecular H-transfer pathway.

We use the geometry optimized crystal structures as the initial configurations for the barrier calculations; the crystallographic structures are taken as starting geometries and then optimized

Table 1
Intramolecular bond lengths and bond angles for the three pure polymorph forms of crystalline HMX

	β (theor.)	β (expt.)	α (theor.)	α (expt.)	δ (theor.)	δ (expt.)
Av. bond lengths						
N–N (equatorial)	1.37	1.373	1.37	1.367	1.36	1.378
N–N (axial)	1.35	1.354	1.37	1.354	1.35	1.351
N–O	1.24	1.228	1.24	1.228	1.24	1.222
C–N	1.39	1.453	1.38	1.453	1.38	1.470
Av. bond angles						
N–N–O	117	116.8	116	117.5	116	117.8
O–N–O	127	126.3	127	124.9	128	124.3
C–N–N	117	117.3	118	118.7	119	119.6
C–N–C	122	123.1	123	121.8	123	119.3
N–C–N	114	111.8	115	111.8	115	111.7

The experimental bond lengths and angles are taken from crystallographic data (see [32] for α, [33] for β, and [34] for δ).

using our ab initio tight-binding approach. Table 1 shows a comparison of our calculated bond lengths and bond angles to that of crystallographic data for the three pure polymorphic forms of crystalline HMX (see [32] for α, [33] for β, and [34] for δ). The bond lengths and bond angles in the experimental and theoretical data are averaged for simplicity. The agreement between both theory and experiment is quite good, with the largest discrepancies occurring for the C–N bond lengths.

The final configuration is the structure created by abstracting hydrogen from one molecule, forming HONO on its adjacent molecule (also a geometry optimized structure). We present the initial and final configurations used in the barrier calculations in Fig. 1 for δ-HMX (left and right figures, respectively). The internal coordinates of the molecule for both the initial and config-uration were optimized with periodic boundary conditions considered. Each optimized simulation
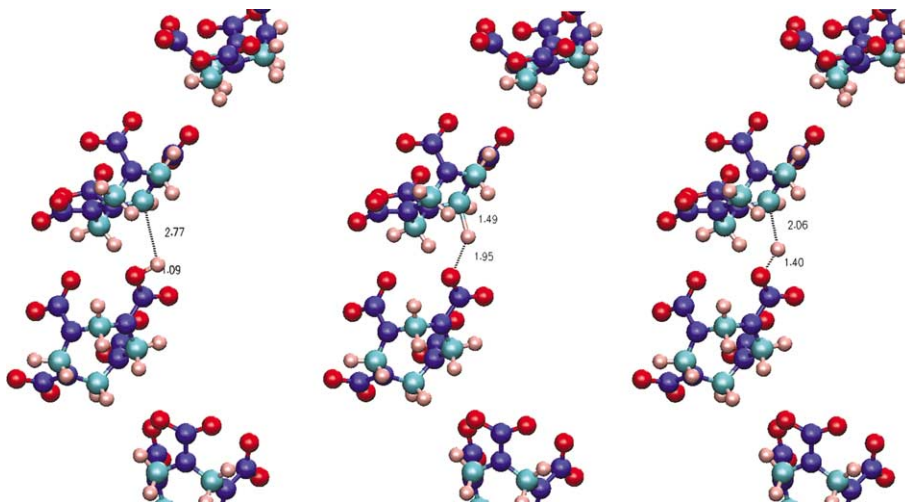

Fig. 1. Snapshots of an intermolecular hydrogen transfer mechanism in δ-HMX. The initial structure (left) is the optimized structure for the δ-HMX phase. With intermolecular hydrogen transfer shown in the intermediate structure (center) formation of HONO on the adjacent molecule is energetically stable (right).
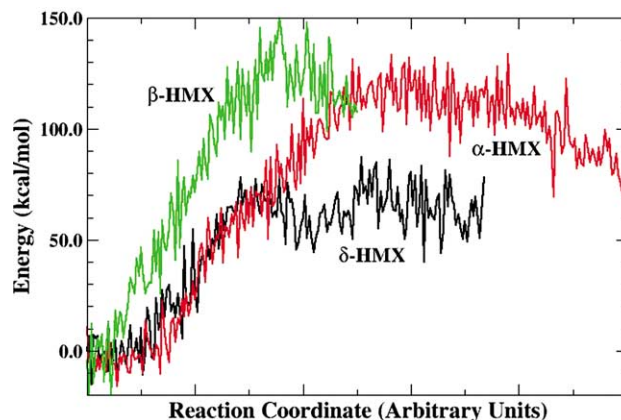

Fig. 2. Energetic profile of intermolecular hydrogen transfer along an arbitrary trajectory (calculated along a path of least resistance) for the three pure polymorphic HMX phases (α, β, and δ).

cell contains six molecules (168 atoms) which is the primitive unit cell of δ-HMX; however, not all molecules are shown. For all calculations, the experimental lattice parameters were used; previous results using FIREBALL indicate that the lattice parameter optimizations for HMX are near experiment [19].

Starting from the initial configuration (left figure in Fig. 1) the atoms are *pushed* to the final configuration (right figure in Fig. 1). The motion of the transferred hydrogen maps out a trajectory along a path of least resistance. An intermediate configuration along this path is shown in Fig. 1 (central figure). We performed barrier calculations for intermolecular hydrogen transfer in condensed-phase α- and β-HMX, similar to the procedure outlined for δ-HMX. But, both α- and β-HMX simulations contained eight molecules (224 atoms) in the super-cell (primitive unit cell size of α-HMX).

The results of the energetics from our three barrier calculations are plotted in Fig. 2. Resultant energies plotted are relative to the optimized initial configuration for each phase. The barrier algorithm gives a trajectory along a path of least resistance; hence, the pathway is not along a specifically defined reaction coordinate. Rather, each point along the plotted *reaction coordinate* represents a point along the trajectory defined by the *pushing* of the initial configuration to the final configuration within the described barrier algorithm. Note that the barrier algorithm of course does not take into account temperature effects, but rather, it gives an energy profile of the reaction along a path of least resistance. The energetics could be refined by considering the addition of the entropic effects through a harmonic approximation; however, that is the scope of future considerations.

The result of our calculations, shown in Fig. 2, indicate that the intermolecular hydrogen transfer has a lower barrier of formation in δ-HMX compared to α- and β-HMX. The fact that this intermolecular hydrogen transfer is more energetic in α-HMX than in β-HMX and more energetic in δ-HMX than in α-HMX is likely connected to the density of each material. We suggest that more volume allows for an energetic conformational

change of the molecule as the HONO formation occurs (the ring diameter of the HONO forming molecule increases slightly). Of all the three pure polymorph phases δ-HMX is significantly the least dense of the three phases, and α-HMX is less dense than β-HMX.

4. Summary

The primary conclusion that we reach from our results is that the energetic trend for intermolecular hydrogen transfer follows the same trend with regards to HMX sensitivity. It is putatively well demonstrated that δ-HMX is more sensitive than β-HMX. Less is known about α-HMX as it is a transition between the other two phases, but it is proposed that α-HMX has sensitivity between β- and δ-HMX. Therefore, our results conclude that the energetic trend, and hence the sensitivity trend, is likely due to the densities; there is more empty volume for the reactions to proceed (i.e., the reduced volume dues to crystal packing hinders conformational changes in the molecules as the intermolecular hydrogen transfer progresses).

An initial understanding of the intermolecular hydrogen transfer which forms HONO within condensed-phase HMX is obtained in this work. These results will provide the basis for further investigative work of condensed-phase HONO elimination, where the free energy of this reaction pathway will be considered using an umbrella sampling technique. Additionally, quantum contributions of this intermolecular hydrogen transfer pathway using path integral techniques will be considered in future work. Most importantly, we demonstrate that energy profiles of condensed-phase HMX reactions are now within reach using local-orbital total-energy methods.

References

[1] R.L. Bishop, D.M. Harradine, R.L. Flesner, S.A. Larson, D.A. Bell, Ind. Eng. Chem. Res. 39 (2000) 1215.

[2] S.B. Hawthorne, A.J.M. Lagadec, D. Kalderis, A.V. Lilke, D.J. Miller, Environ. Sci. Technol. 34 (2000) 3224.

[3] G.T. Long, S. Vyazovkin, B.A. Brems, C.A. Wight, J. Chem. Phys. B 104 (2000) 2570.

[4] N.J. Harris, K. Lammertsma, J. Am. Chem. Soc. 119 (1997) 6583.

[5] C. Wu, L.E. Fried, J. Phys. Chem. A 101 (1997) 8675.

[6] S. Zhang, T.N. Truong, J. Phys. Chem. A 104 (2001) 2427.

[7] J.P. Lewis, K.R. Glaesemann, K. VanOpdorp, G.A. Voth, J. Phys. Chem. A 104 (2000) 11384.

[8] D. Chakraborty, R.P. Muller, S. Dasgupta, I.W.A. Goddard, J. Phys. Chem. A 105 (2001) 1302.

[9] T.D. Sewell, D.L. Thompson, J. Phys. Chem. 95 (1991) 6228.

[10] C.C. Chambers, D.L. Thompson, J. Phys. Chem. 99 (1995) 15881.

[11] Y. Kohno, K. Ueda, A. Imamura, J. Phys. Chem. 100 (1997) 4701.

[12] Y. Guo, D.L. Thompson, J. Phys. Chem. B 103 (1999) 10599.

[13] M.M. Kukla, J. Phys. Chem. B 105 (2001) 10159.

[14] M.R. Manaa, L.E. Fried, C.F. Melius, M. Elstner, T. Frauenheim, J. Phys. Chem. B (2002).

[15] P. Politzer, J.S. Murray, P. Lane, P. Sjoberg, H.G. Adolph, Chem. Phys. Let. 181 (1991) 78.

[16] C.B. Skidmore, D.S. Phillips, D.J. Idar, S.F. Son, Characterizing the microstructure of selected high explosives, in: Europyro 99 vol. I, pages 2–10, Association Francaise de Pyrotechnie, Brest, France, June 7–11, 1999.

[17] D.J. Idar, R.A. Lucht, J.W. Straight, R.J. Scammon, R.V. Browning, J. Middleditch, J.K. Dienes, C.B. Skidmore, G.A. Buntain, Low amplitude insult project: Pbx 9501 high explosive violent reaction experiments, in: Proceedings of the Eleventh International Detonation Symposium: Snowmass Village, CO, Aug 31–Sept 4, 1999, page 335 Naval Surface Warfare Center, Indian Head, 1999.

[18] B.M. Rice, G.F. Adams, M. Page, D.L. Thompson, J. Phys. Chem. 99 (1995) 5016.

[19] J.P. Lewis, T.D. Sewell, R.B. Evans, G.A. Voth, J. Phys. Chem. B 104 (2000) 1009.

[20] J.P. Lewis, H. Chevreau, G.A. Voth, J. Phys. Chem. A (submitted).

[21] P.A. Lofy, PhD thesis, Department of Chemistry, University of Utah, Salt Lake City, Utah, 1999.

[22] J.P. Lewis, K.R. Glaesemann, G.A. Voth, J. Fritsch, A.A. Demkov, J. Ortega, O.F. Sankey, Phys. Rev. B 64 (2001) 195103.

[23] A.A. Demkov, J. Ortega, O.F. Sankey, M.P. Grumbach, Phys. Rev. B 52 (1995) 1618.

[24] A. Horsfield, Phys. Rev. B 56 (1997) 6594.

[25] A.D. Becke, Phys. Rev. A 38 (1988) 3098.

[26] C. Lee, W. Yang, R.G. Parr, Phys. Rev. B 37 (1988) 785.

[27] D.R. Hamann, Phys. Rev. B 40 (1989) 2980.

[28] M. Fuchs, M. Scheffler, Comp. Phys. Commun. 119 (1999) 67.

[29] L. Kleinman, D.M. Bylander, Phys. Rev. Lett. 48 (1982) 1425.

[30] M. Finnis, J. Phys.: Condens. Mat. 2 (1990) 331.

[31] B. Delley, J. Chem. Phys. 92 (1990) 508.

[32] H.H. Cady, A.C. Larson, D.T. Cromer, Acta Cryst. 16 (1963) 617.

[33] C.S. Choi, H.P. Boutin, Acta Cryst. B 26 (1970) 1235.

[34] R.E. Cobbledick, R.W.H. Small, Acta Cryst. 30 (1974) 1918.